Electrochimica Acta 178 (2015) 739–747

Contents lists available at ScienceDirect

Electrochimica Acta

journal homepage: www.elsevier.com/locate/electacta

Electrocatalysis of the hydrogen evolution reaction by rhenium oxides electrodeposited by pulsed-current

Alejandro Vargas-Uscategui[a,*, 1], Edgar Mosquera[b], Boris Chornik[c], Luis Cifuentes[a]

[a] Laboratorio de Electrometalurgia, Departamento de Ingeniería de Minas, Facultad de Ciencias Físicas y Matemáticas, Universidad de Chile, Tupper Av. 2069, Santiago, Chile
[b] Laboratorio de Materiales a Nanoescala, Departamento de Ciencia de los Materiales. Facultad de Ciencias Físicas y Matemáticas, Universidad de Chile, Tupper Av. 2069, Santiago, Chile
[c] Departamento de Física, Facultad de Ciencias Físicas y Matemáticas, Universidad de Chile, Casilla 487-3, Santiago 8370415, Chile

ARTICLE INFO

Article history:
Received 29 April 2015
Received in revised form 5 August 2015
Accepted 13 August 2015
Available online 17 August 2015

Keywords:
Rhenium oxide
pulsed current electrodeposition
electrocatalysis
hydrogen evolution reaction
cyclic voltammetry

ABSTRACT

Rhenium oxides are materials of interest for applications in the catalysis of reactions such as those occurring in fuel cells and photoelectrochemical cells. This research work was devoted to the production of rhenium oxide by means of pulsed current electrodeposition for the electrocatalysis of the hydrogen evolution reaction (HER). Rhenium oxides were electrodeposited over a transparent conductive oxide substrate (Indium Tin-doped Oxide – ITO) in an alkaline aqueous electrolyte. The electrodeposition process allowed the production of rhenium oxides islands (200–600 nm) with the presence of three oxidized rhenium species: Re^{IV} associated to ReO_2, Re^{VI} associated to ReO_3 and Re^{VII} associated to $H(ReO_4)$ H_2O. Electrodeposited rhenium oxides showed electrocatalytic behavior over the HER and an increase of one order of magnitude of the exchange current density was observed compared to the reaction taking place on the bare substrate. The electrocatalytic behavior varied with the morphology and relative abundance of oxidized rhenium species in the electrodeposits. Finally, two mechanisms of electrocatalysis were proposed to explain experimental results.

1. Introduction

Rhenium oxides are of interest in industrial and technological applications. Re_2O_7, ReO_3 y ReO_2 have been mostly used in heterogeneous catalysis and fuel cells [1,2]. Recently there has been an increased interest in applying these oxides to electrochromic devices [3], liquid crystal cells [1], fuel cells [4–6], and photoelectrochemical cells [7–9]. This is because their cost is lower than that of other materials, such as Pt, Pd or Rh.

In fuel cells and photoelectrochemical cells it is expected that electrode materials exhibit the capability of sustaining high current densities with low over potentials, which is to say, high process rates [10,11]. In particular, ReO_2 has proved capable of activating the hydrogen evolution reaction (HER), with a behavior similar to that of a Pt electrode [12,13].

This work deals with tuning process conditions for the production of Re oxides for electrocatalytic applications such as HER. A quick pulsed electrodeposition process (able to produce the desired results in about 5 minutes) is proposed to develop materials with the required surface characteristics (morphology and composition) for the electrocatalysis of the HER. Re-oxides were electrodeposited on Indium Tin-doped Oxide (ITO) from an alkaline electrolyte in order to test the potential of these materials for the production of H_2. This paper also aims to show the efforts in understanding the electrocatalysis mechanism of the HER over Re-oxides, making emphasis in the underlying importance of the type of rhenium oxide. It is necessary to point out that, to date, no evidence has been presented in the scientific literature for the pulsed-current electrodeposition of Re oxides.

2. Experimental details

2.1. Preparation of samples

Table 1 shows the experimental conditions that were studied in this research. Experimental work to study the electrocatalytic behavior of rhenium oxides was carried out by preparing a set of solutions formed by reagent-grade ammonium perrhenate

* Corresponding author. Tel.: +56 2 978 4795/978 4222; fax: +56 2 699 4119.
E-mail addresses: avargasuscat@ing.uchile.cl (A. Vargas-Uscategui), luicifue@cec.uchile.cl (L. Cifuentes).
[1] Present Addresses: CSIRO Chile International Centre of Excellence, Tupper Av. 2007, Santiago, Chile

http://dx.doi.org/10.1016/j.electacta.2015.08.065
0013-4686/

Table 1
Experimental conditions for the pulsed current electrodeposition of rhenium oxides.

Experiment	NH_4ReO_4 [mol dm^{-3}]	NaOH [mol dm^{-3}]	H_2SO_4 [mol dm^{-3}]	pH	Cathodic parameters		Anodic parameters	
					Ic [10^{-3} A]	tc [10^{-3} s]	Ic [10^{-3} A]	tc [10^{-3} s]
1	0.02 ± 0.001	0.90 ± 0.04	0.45 ± 0.02	8.49 ± 0.01	1	100	1	10
2					5	100	1	10
3	0.04 ± 0.002	0.90 ± 0.04	0.45 ± 0.02	8.45 ± 0.01	1	100	1	10
4					5	100	1	10

(NH_4ReO_4, Molymet S.A.), high purity sodium hydroxide (NaOH, Sharlau), sulphuric acid (98% H_2SO_4, Merck) and deionized water (Barnestead, Nanopure, 18 MΩ cm) at room temperature. These solutions were used as electrolytes to produce rhenium oxides by means of pulsed current electrodeposition, which were carried out under a variety of selected conditions. Rhenium concentration in solution was checked by optical inductively coupled plasma with a Perkin Elmer Optima 5300DV unit. pH was measured after 12 h prior to the electrodeposition at 25 ± 1 °C with a Schott Prolab 1000. There was no observed precipitation of salt crystals or any other sediment from the electrolyte.

The electrodeposition of rhenium oxides was carried out in a standard double jacket-glass electrochemical cell with two electrodes (anode and cathode). A cathode of conductive indium tin-doped oxide (ITO)-coated glass (Aldrich, 8–12 Ω sq^{-1}) and anodes of platinum (Pt, 99.9%) with an apparent surface area of 1.0 cm^2 and 4.0 cm^2 were used. The ITO-coated glass substrates were cleaned by sonication for 5 min in various solutions: a) acetone, b) ethanol, c) H_2O_2 and d) deionized water. Then the substrates were dried in warm air. The platinum anode was immersed in a 1:1 sulpho nitric solution (5 mol dm^{-3} H_2SO_4 + 5 mol dm^{-3} HNO_3) for 60 s, then immersed in H_2O_2 for 120 s and finally rinsed with deionized water. The anode-cathode separation was 10 mm.

The pulsed current electrodeposition was conducted in a reverse pulsing power supply (model WSe5-10/12, Novak Technologies); discrete values of the cell potential in the range 0.75–2.75 V were recorded with the use of the power supply. All the experiments were made to a total deposition time of 300 s. A thermostat bath (Lauda Eco Gold RE415) was used to keep the temperature at 25 ± 0.5 °C inside the double jacket-glass cell and a continuous bubbling of N_2 was used to eliminate the oxygen in solution, while stirring at 1200 rpm. The system was kept inside a house-made Faraday cage in order to prevent electromagnetic interference.

The ITO-coated glasses were copiously rinsed with deionized water after the electrodeposition process. The films were desiccated and heated in an argon atmosphere at a rate of 2 °C/min to a final temperature of 180 °C and held for 2 h; the cooling was made inside the oven in an argon atmosphere. Detachment of the electrodeposited material was not observed. The resulting films were compositionally homogeneous and were stored in a desiccator for one week prior to characterization and further analysis.

2.2. Materials characterization

The electrodeposited materials were examined with a FEI-Quanta 250 FEG-ESEM scanning electron microscope (SEM) operated at 20 kV. An Oxford Instruments Energy Dispersive X-Ray (EDX) detector is attached to the SEM which allows the chemistry of the samples to be investigated on the micron and sub-micron scale; several readings were taken for each measurement over sections of 240 × 240 μm^2 and the reported values are averages.

X-ray photoelectron spectroscopy (XPS) measurements were carried out using a Perkin Elmer PHI 1257 electron spectrometer. Non-filtered Al-Kα radiation (hν = 1486.6 eV) was used as excitation source. The take-off angle of the emitted photoelectrons was set to 45° with respect to the sample surface normal. The data were obtained at room temperature and typically the operating pressure in the analysis chamber was maintained at ca. 10^{-7} Pa. Internal calibration of the binding energy (BE) of the spectra was made by using the C-1*s* line of adventitious carbon, setting it at 284.8 eV. The accuracy of the BE scale was ±0.1 eV. High resolution spectra of Re 4*f* electronic transitions were taken and averaged during data acquisition. In order to accurately determine the BE of the different element core levels, high resolution spectra were always fitted using Voigt functions. A background curve was subtracted by the method devised by Shirley [14]. Spectra were handled and fitted using UNIFIT software. The following criteria were employed to analyze Re spectra: i) the area of the $4f_{5/2}$ peak was constrained to be 75% of the $4f_{7/2}$ peak area; and ii) both peaks were set to have the same shape and the same full-width at half maximum (FWHM).

2.3. Electrochemical characterization

The electrocatalytic behavior of rhenium oxides electrodeposited by pulsed current for the hydrogen evolution reaction was studied by means of cyclic voltammetry (CV). For the CV experiments, a three-electrode system was employed with platinum as a counter electrode and an Ag/AgCl/KCl (saturated) reference electrode. All potentials are referred to this electrode. Re oxides electrodeposited by pulsed current over ITO substrates were used as working electrodes for the electro catalytic study. The geometric area of the electrode (1.0 cm^2) was used as a reference for the density current. The electrolyte was an acidic aqueous solution at pH 0.38 ± 0.01 (0.5 mol dm^{-3} H_2SO_4) in deionized water (Barnestead, Nanopure, 18 MΩ cm). The experiments were made in static conditions after a purge for 15 minutes with N_2; an atmosphere of the same gas was kept over the solution during the experiment to avoid an excessive presence of oxygen. Measurements were conducted at 25 ± 0.1 °C. The cyclic voltammograms were recorded with a radiometer PGZ301 potentiostat-galvanostat controlled by a PC equipped with Voltamaster 4 software. The analysis region during the experiment covered the range +0.5 V to −0.5 V vs. Ag/AgCl/KCl and the scanning rate was between 0.005 V s^{-1} and 0.5 V s^{-1}. Dynamic ohmic drop compensation was performed during data acquisition by using a function available in the electrochemical interface. The system was kept inside a house-made Faraday cage in order to prevent electromagnetic interference. The scans were run from anodic to cathodic potentials and three experiments were run for every condition in order to ensure reproducibility. Exchange current density (j_o) and charge transfer coefficient (α) were calculated considering the high-field approximation to the Butler-Volmer equation [15,16]. The parameters j_o and α were obtained by a linear

fitting of the experimental data using OriginPro v. 8.1 software with a correlation coefficient (R^2) higher than 0.99 and a chi-squared (χ^2) value lower than 5.

3. Results and discussion

Fig. 1 shows SEM images of the rhenium oxides electrodeposited by pulsed current over ITO substrates; brighter zones corresponded to the electrodeposits whereas darker zones corresponded to the substrate. SEM analysis showed that the size of electrodeposited islands was less that 600 nm. The latter is a result of a deposition time (300 s) that prevented the formation of a dense thin film on the ITO substrate thus having a low impact on the transparency of the substrate after the electrodeposition of Re oxides. Also, it is important to note that dispersion and distribution of the islands of Re oxides depend on process conditions.

In the described process conditions, an increase in ReO_4^- ions concentration caused an increasing of the amount of electrodeposited material as well as the size of the observed nuclei. On the other hand, increasing the process current density caused a decrease in nuclei size. The first effect was the result of an improvement in the electrodeposition rate, given that a greater amount of ReO_4^- ions in solution enhanced the mass transport in the electrolyte, thus increasing the amount of ions being reduced on the cathode surface. The second effect may be explained by considering that an increase in the cathodic current density favored a progressive nucleation rather than an instantaneous one. This meant that, at a current density of 50 A m^{-2} the material tends to form small islands that gradually occupy the free sites on the substrate surface without overlapping, whereas, at a current density of 10 A m^{-2} the material tends to grow on previously formed nuclei. The effect of nucleation type (instantaneous or progressive) influences the growth type and, as a result, the generated structures. Due to this effect, it is possible to state that the material presents well-defined facets, which suggests the formation of a crystalline compound based on Re oxides. The adopted forms are important because they generate electrochemically active zones, which will be important for ion intercalation (H^+).

As to the electrodeposition mechanism, it is necessary to consider that the reduction sequence from perrhenate ion (ReO_4^-) to Re (VI) oxide, Re (IV) oxide or metallic Re is affected by the presence of the HER [17,18]. The latter is faster than ReO_4^- reduction, which negatively affects the faradic efficiency of the process, but may help controlling nuclei growth by confining the electrocrystallization reaction to the spaces left between the bubbles of generated hydrogen, thus limiting nuclei growth. However, nuclei growth control through the HER may be a great challenge. This is due to the great difference in species concentrations (water is the solvent, whereas the solute is between 0.02 mol dm^{-3} and 0.04 mol dm^{-3}) and also to the fact that the electrodeposited Re species may catalyze the same HER. SEM observations allow the following statement: a correct combination of electrodeposition parameters in alkaline solution may produce tailor-made materials based on Re oxides.

The surface of the electrodeposited materials was analyzed by means of energy dispersive spectrometry (EDS) and the results for elemental chemical composition are shown in Table 2. The latter contains composition data for Re, In, Sn and O measured in $240 \times 240\ \mu m^2$ sections. Elements which are contained by the substrate's glass (Si-SiO_2, Na-Na_2SO_4, Ca-CaO, Mg-MgO y Al-Al_2O_3) were excluded from the calculation matrix. As to the elements which are contained in the ITO substrate, it is necessary to consider that their variation is related to the calculation matrix; this does not imply that elements such as In or Sn are lost. It is possible to determine the effect of process variables not only on material morphology, but also on the Re concentration found on the surface. The concentration of the ReO_4^- ions in solution influences the

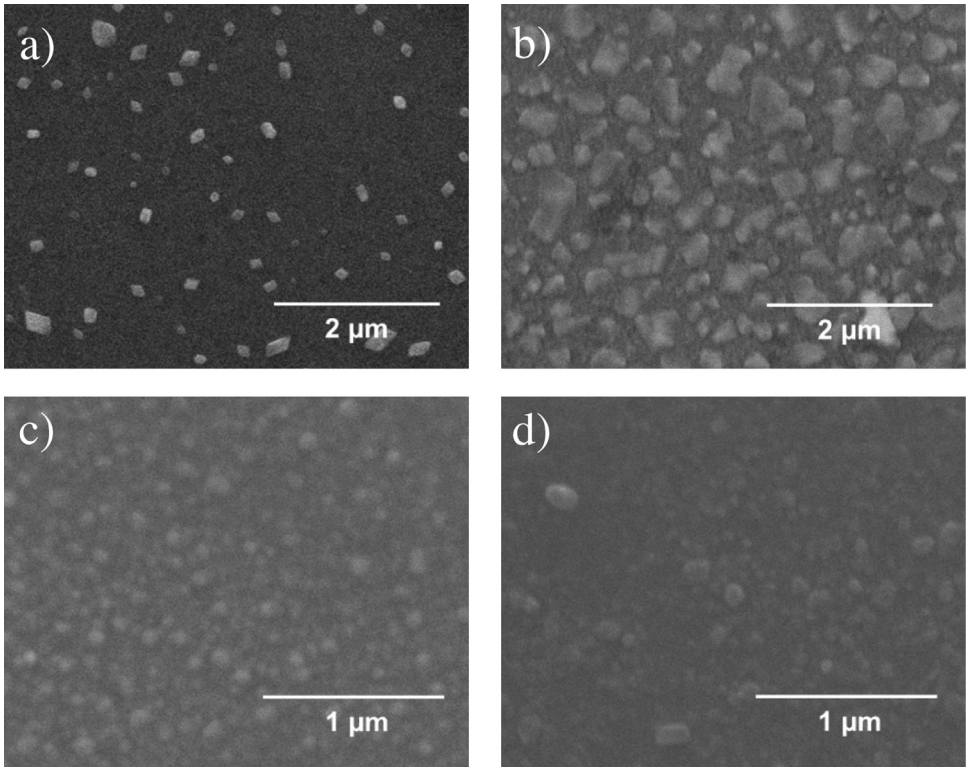

Fig. 1. SEM images of rhenium oxides electrodeposited by pulsed current over ITO substrate obtained at different process conditions: a) 0.02 mol dm^{-3} ReO_4^- @ 10 A m^{-2}; b) 0.04 mol dm^{-3} ReO_4^- @ 10 A m^{-2}; c) 0.02 mol dm^{-3} ReO_4^- @ 50 A m^{-2}; and d) 0.04 mol dm^{-3} ReO_4^- @ 50 A m^{-2}.

Table 2
Surface chemical composition of the electrodeposits on the ITO substrate (Average concentration, wt%).

Electrodeposit	Electrolyte	Cathodic Parameter	Re	In	Sn	O	Total
1	(0.02 mol dm^{-3} ReO_4^-)	(jc = 10 A m^{-2})	5 ± 2	73 ± 3	10 ± 2	12 ± 2	100
2		(jc = 50 A m^{-2})	5 ± 1	70 ± 2	11 ± 2	14 ± 1	100
3	(0.04 mol dm^{-3} ReO_4^-)	(jc = 10 A m^{-2})	7 ± 3	73 ± 3	12 ± 2	8 ± 2	100
4		(jc = 50 A m^{-2})	10 ± 2	68 ± 2	11 ± 2	11 ± 2	100
	Bare ITO		–	72 ± 3	14 ± 2	14 ± 3	100

amount of Re in the deposit, due to a greater mass of ions available for reduction on the ITO surface. Equally, a cathodic current density of 50 A m^{-2} determines an increase in the amount of deposited Re, which is in agreement with Faraday's law.

However, it should be noticed that the magnitude of the effect of process parameters on the Re concentration in the deposit varies. An increase in perrhenate concentration causes a greater increase of Re in the deposit than an increase in cathodic current density. This is caused by the fact that an increase in ReO_4^- concentration in solution favors the mass transport rate, whereas an increase in the cathodic current density, apart from accelerating the reduction of ReO_4^-, also makes the HER rate greater. In process terms, this means that, to favor the incorporation of Re in the deposit, the increase in perrhenate concentration should be privileged, instead of that of the cathodic current. This is to hinder an excessive reduction in the cathodic efficiency, apart from problems associated with hydrogen adsorption and fragilization by hydrogen.

In Fig. 2, the high-resolution XPS spectra for the Re 4*f* shell of various materials electrodeposited on an ITO substrate are shown. The distribution of Re oxidation states on the surface of the electrodeposited materials is also shown in this figure. This distribution was estimated by adjustment of the spectrum curves. In particular, the spectra show the characteristic $4f_{7/2}$ and $4f_{5/2}$ Re doublets. The best adjustment of Voigt functions was obtained by using six components belonging to three Re valences. Three oxidized Re species were identified: a) near 41.9 ± 0.1 eV, b) near 43.7 ± 0.2 eV, and c) near 46.1 ± 0.2 eV. These values showed a chemical shift near 1.5 eV, 3.3 eV and 5.8 eV, with respect to metallic Re $4f_{7/2}$ (40.31 ± 0.06 eV). The peak at 41.9 eV was assigned to Re^{IV} in the ReO_2 compound [19,20], the peak at 43.7 eV was assigned to Re^{VI} in the ReO_3 compound [19,21], and the peak at 46.1 eV was assigned to Re^{VII} in the $H(ReO_4)H_2O$ compound [21–23].

According to the previously reported electrodeposition mechanism [18], the electrocrystallization process of Re oxides in aqueous alkaline solution may advance towards the gradual formation of intermediate oxides in the $Re^{VII} \leftrightarrow Re^{VI} \leftrightarrow Re^{IV}$ sequence. According to XPS analysis, the principal species that coexist on the surface of the electrodeposited material were Re^{IV}, Re^{VI} and Re^{VII}. The Re^{IV} and Re^{VI} species are expected in the system, but the Re^{VII} species arises from aging of the material as a result of its interaction with the environment [23].

Table 3 summarizes the values of photoelectron lines for Re found in high-resolution spectra and the corresponding FWHM, apart from values for the relative abundances for each Re species as

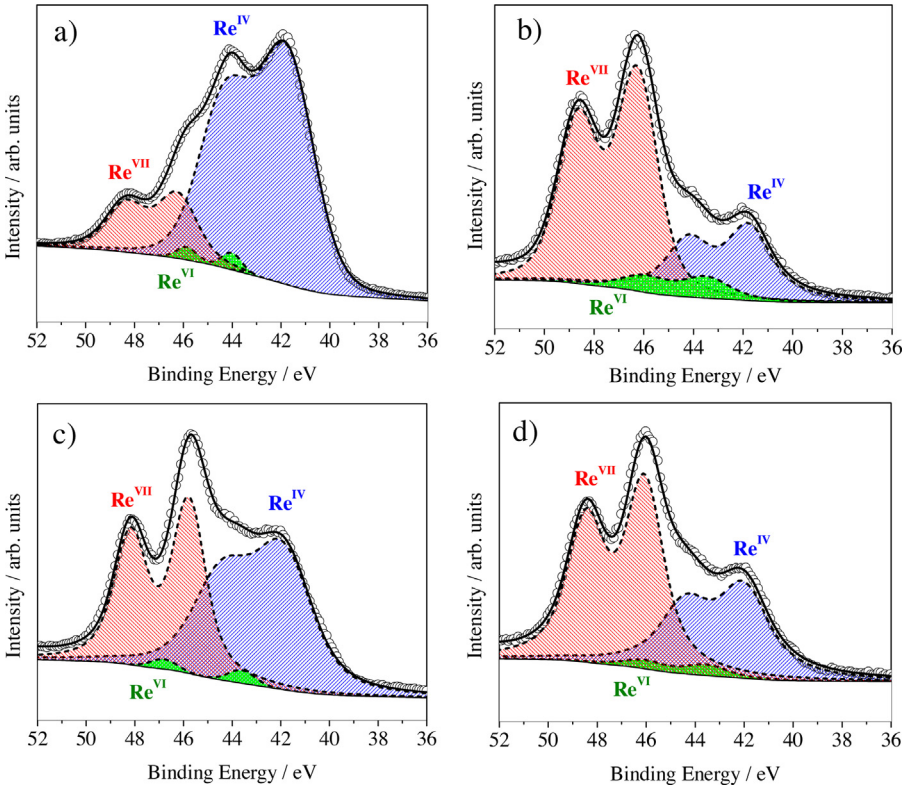

Fig. 2. High-resolution XPS spectra of the Re 4*f* core levels for the electrodeposited Re oxides on ITO substrate at different process conditions: a) 0.02 mol dm^{-3} ReO_4^- @ 10 A m^{-2}; b) 0.04 mol dm^{-3} ReO_4^- @ 10 A m^{-2}; c) 0.02 mol dm^{-3} ReO_4^- @ 50 A m^{-2}; and d) 0.04 mol dm^{-3} ReO_4^- @ 50 A m^{-2}. The thicker line is the fitting of the experimental data (open circles) by Voigt functions (dotted lines).

Table 3
Binding energy of the Re 4*f* photoelectron lines and relative abundances of Re^{VII}, Re^{VI} and Re^{IV} species on the electrodeposit surface. (*) All energies are referred to the C 1*s* photoelectron line (284.8 eV). (**) Figures in brackets represent the FWHM of the peak.

Photoelectron line (*)	Species	Electrolyte - 1 0.02 mol dm^{-3} ReO_4^-		Electrolyte - 2 0.04 mol dm^{-3} ReO_4^-	
		Process Condition - A jc = 10 A m^{-2}	Process Condition - B jc = 50 A m^{-2}	Process Condition - A jc = 10 A m^{-2}	Process Condition - B jc = 50 A m^{-2}
Re $4f_{7/2}$ (eV) (**)	Re (IV)	41.7 (2.6)	41.9 (2.9)	41.8 (2.2)	42.0 (2.5)
	Re (VI)	44.0 (1.0)	43.6 (1.3)	43.5 (2.3)	43.5 (2.0)
	Re (VII)	46.2 (2.0)	45.8 (1.7)	46.3 (2.0)	46.1 (1.9)
Re $4f_{5/2}$ (eV) (**)	Re (IV)	44.2 (2.6)	44.4 (2.9)	44.2 (2.2)	44.4 (2.5)
	Re (VI)	45.9 (1.0)	46.8 (1.3)	46.0 (2.3)	46.1 (2.0)
	Re (VII)	48.3 (2.0)	48.2 (1.7)	48.6 (2.0)	48.5 (1.9)
Re (IV)	77.0 %	54.4 %	27.2 %	37.4 %	
Re (VI)	1.8 %	2.2 %	7.7 %	3.7 %	
Re (VII)	21.3 %	43.4 %	65.1 %	58.8 %	
		100.0 %	100.0 %	100.0 %	100.0 %
Re(IV): Re (VII)	3.6: 1	1.3: 1	0.4: 1	0.6: 1	

a function of the electrodeposition process conditions. The differences between the values reported in the literature and those experimentally determined by the authors may be explained considering that the electrodeposited material is composed of a mixture of Re oxides of various valences. As a result, the binding energy may vary as a function of the closest neighbors, which modify the electronic environment surrounding each site [21,24]. Additionally, the differences in Re oxidation states on the surface and the FWHM of the peaks could be an indication that the electrodeposited material is a mixture of oxides of various valences that are not fully integrated with each other. This condition implies that both oxidized Re compounds may be separated but distinguishable by their structure (amorphous or crystalline). It is important to stress that the values for the FWHM for the Re^{VII} species are lower than those for the Re^{IV} species, which probably indicates that the first species exhibits a greater crystallinity than the second one [25].

The species Re^{IV}, Re^{VI} and Re^{VII} present the same factor of atomic sensitivity and, as a result, it is possible to calculate the relative abundance of each Re species. This is the basis for a comparison of the variation of the Re^{IV}: Re^{VII} ratio for each one of the electrodeposition conditions, as shown in Table 3; the relative abundance of Re^{VI} is significantly lower by comparison with the other two species and therefore can be consider that would not play a determinant role in the electrocatalysis mechanism. The variation in the amount of the Re^{VII} species is linked to the relative concentration of the species which produce it. In agreement with this, and with the fact that the $H(ReO_4)H_2O$ compound is not an expected product of the electrodeposition (as it arises from the interaction between the Re^{IV} and Re^{VI} species and their environment), it is possible to infer indirectly that the material which electrodeposits on ITO contains the species mentioned in the previously proposed mechanism [18,23]. When comparing the relative surface abundances Re^{IV}: Re^{VII} for each process condition, as shown on Table 3, it becomes clear that an increase in ReO_4^- ion concentration in the electrolyte reduces the relative abundance of the ReO_2 compound. This situation also arises when the cathodic current density increases. Both factors may be the result of the formation of a greater amount of both Re^{IV} and Re^{VI} species. Their interaction with the environment leads to a greater surface formation of the $H(ReO_4)H_2O$ compound.

Fig. 3 shows cyclic voltammograms representative of the materials being studied (ITO and Re oxide electrodeposits) obtained at a 200 mV s^{-1} sweep rate. In particular, it is possible to state a low reaction rate of the HER on ITO with values above −0.02 A m^{-2} at a potential of −0.4 V vs. Ag/AgCl/KCl. Considering this, it is possible to state that the ITO surface presents a behavior similar to an ideally polarizable electrode where there is no charge

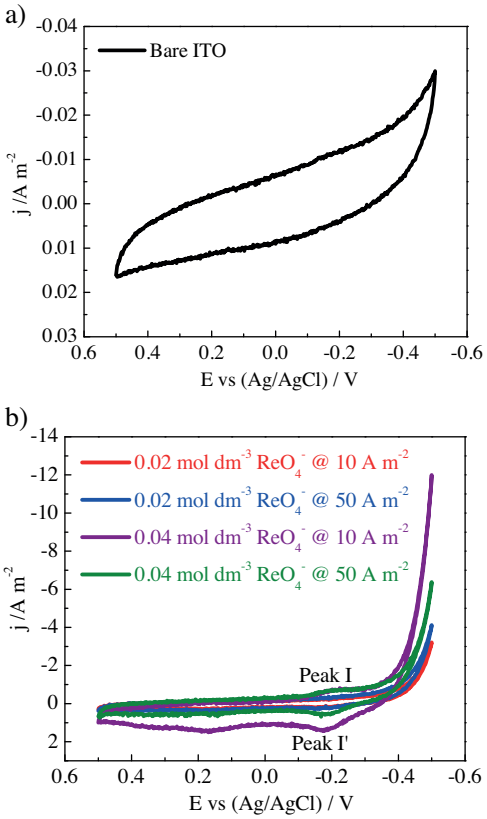

Fig. 3. Voltammograms measured in 0.5 mol dm^{-3} H_2SO_4 solutions on: a) bare ITO, and b) rhenium oxides electrodeposited by pulsed current obtained at various process conditions (Scan rate ν = 200 mV s^{-1}).

transfer through the electrode/electrolyte interface and leading to a low HER rate. The low HER rate is also linked to a low H^+ adsorption on the ITO surface [26].

On the other hand, when analyzing the HER rate on the electrodeposited materials, it is possible to state in the first instance that the values on the current density axis are significantly higher than in the case of the substrate without deposit; for instance, for a potential of −0.4 V vs. Ag/AgCl/KCl, the current density is of the order of 40 to 100 times greater. The increase in the HER is then the product of the presence of Re oxides that contribute the observed electrocatalytic effect.

As to the possibility of electrochromism, it is necessary to point out that none of the samples exhibited color changes during the

cyclic voltammetry tests. The transparency of the system (substrate + electrodeposit) was maintained throughout, which supports the statements made in [27], i.e. electrodeposited rhenium oxides did not exhibited electrochromic behavior. Neither physical nor electrochemical changes were observed during recording voltammograms that could indicate the dissolution/deposition of the rhenium oxides.

The electrocatalytic effect is noticeable in the electrodeposited Re oxide materials, but it is necessary to stress that the mechanism through which it accelerates the HER is different for each one of the studied materials. Those electrodeposits arising from a 0.02 mol dm^{-3} ReO_4^- electrolytes at 10 and 50 A m^{-2} exhibited exponential curves typical of a process under charge transfer control. This could indicate that the step previous to proton adsorption (H^+_{ad}) does not involve intercalation in the solid, which suggests that the electrocatalysis process is mainly controlled by electron transfer on the surface of the electrodeposited material. The said control is primordially associated to the Re species which interacts in the electrolyte-surface interface during the HER, therefore, considering that these deposits exhibited strong XPS photoelectron signals associated to Re^{IV} in ReO_2, it is possible to state that this species is dominant in the electrocatalysis phenomenon. This statement is also founded in the fact that, in the ReO_2 structure, each metallic center is coordinated with at least six O atoms and two Re atoms (a structure of the disordered rutile type), which allows better electron transfer for the HER.

Under these assumptions, it is possible to propose an electrocatalysis mechanism for the HER where the first step requires reduction of the metallic center according to Eq. (1) (see below), which causes the loss of a positive charge from the solid structure. This may lead to the surface adsorption of a proton, as shown in Eq. (2). The H^+_{ad} species may interact with a homologous species to form molecular hydrogen (H_2) and regenerate the catalyst, as shown in Eq. (3). It is necessary to mention that these reactions take place simultaneously to the reaction shown in Eq. (4).

$$(Re^{IV}O_2)_{(s)} + e^- \rightarrow (Re^{III}O_2)^-{}_{(s)} \quad (1)$$

$$(Re^{III}O_2)^-{}_{(s)} + H^+ \rightarrow (H^+_{ad}Re^{III}O_2)_{(s)} \quad (2)$$

$$2(H^+_{ad}Re^{III}O_2)_{(s)} \rightarrow 2(Re^{IV}O_2)_{(s)} + H_{2(g)} \quad (3)$$

$$2H^+ + 2e^- \leftrightarrow H_2 \quad (4)$$

On the other hand, those materials that were electrodeposited from an electrolyte with a concentration of 0.04 mol dm^{-3} ReO_4^- at 10 y 50 A m^{-2}, also showed a kinetic behavior where the HER was charge transfer controlled. However, in these cases the voltammograms also revealed the presence of a cathodic peak (Peak I) with its corresponding anodic peak (Peak I') as shown in Fig. 3. Figs. 4 and 5 show values for the potential (Ep vs ν, ν being the sweep rate) and current density (jp vs $\nu^{1/2}$) for the cathodic peak (Peak I) and the anodic peak (Peak I') for the materials being considered. These values were determined at a sweep rate (ν) between 50 and 500 mV s^{-1}, given that, at lower values (5, 10 and 20 mV s^{-1}) the system proceeds under charge transfer control; as a result, the peaks (I and I') were not observed. The values determined for electrodeposited materials in an electrolyte with a concentration of 0.04 mol dm^{-3} ReO_4^- at 10 and 50 A m^{-2}, exhibit the same tendency. Hence, it is possible to infer by direct comparison that their magnitudes are statistically similar.

In the case of the cathodic peak it was observed that the potentials ($E_{p,c}$) shifted to more negative values as a consequence

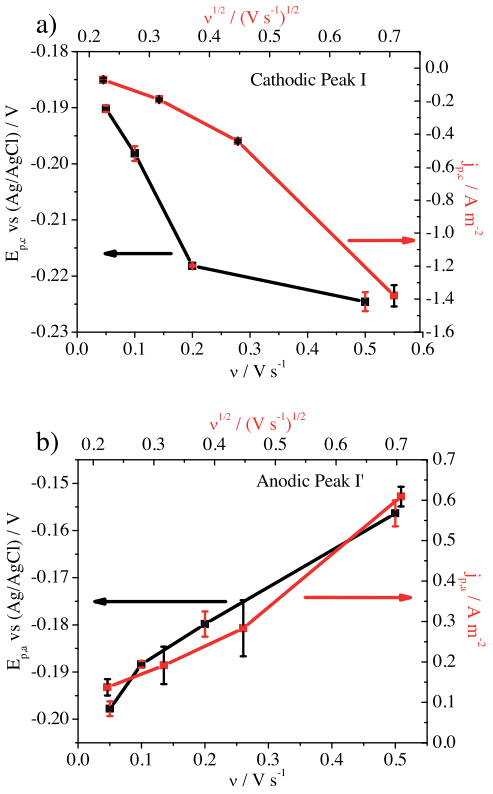

Fig. 4. Values for the cathodic peak I and anodic peak I' of rhenium oxides, electro deposited by pulsed current using an electrolyte with 0.04 mol dm^{-3} ReO_4^- @ 10 A m^{-2}. Peak potential (E_p vs (Ag/AgCl)) as a function of scan rate (ν) and peak current density (j_p) as a function of square root of scan rate ($\nu^{-1/2}$). The voltammograms were recorded in 0.5 mol dm^{-3} H_2SO_4 electrolytes at 25 °C.

of an increase in sweep rate (ν), whereas the current density ($j_{p,c}$) grows with increasing sweep rate (ν). On the other hand, in the case of the anodic peak, the potentials ($E_{p,a}$) show a tendency to be less negative with increasing current density ($j_{p,a}$). Given these characteristics and their dependence on the sweep rate, it is possible to establish that the cathodic peak (Peak I) and the anodic one (Peak I') follow a quasi-reversible process, influenced by mass transport [28].

Considering the presence of a quasi-reversible reaction influenced by mass transfer kinetics in solid state, and given that the peaks are sited in a region close to the HER, this electrochemical process is assigned to proton adsorption (H^+_{ad}) on the electrodeposited material. The peaks I and I' have similar characteristics than the ones found in metallic and metallic alloys that are capable of absorbing H, therefore this could be considered as a proof of the presence of a characteristic under-potential adsorbed hydrogen (H_{UPD}) species on the Re oxides electrode. A difference was established between the materials which were electrodeposited at a concentration of 0.02 mol dm^{-3} ReO_4^- and those electrodeposited at 0.04 mol dm^{-3} ReO_4^-. XPS photoelectron signals associated to Re^{VII} in $H(ReO_4)H_2O$, were found to have higher intensity than the signals of Re^{IV} in ReO_2. This oxide presents the highest Re oxidation state and a crystalline structure formed by tetrahedra $(ReO_4)^-$, which would have enough space for (H^+_{ad}) ions intercalation.

Previously, an electrocatalysis mechanism was proposed, which was based on the greater action of the Re^{IV} species in ReO_2. In this case, the metallic centers of $(ReO_4)^-$ are not directly coordinated with metallic Re, therefore, the mechanism should contemplate the action of isolated metallic centers which function independently. As a result, it is possible to propose an electrocatalysis

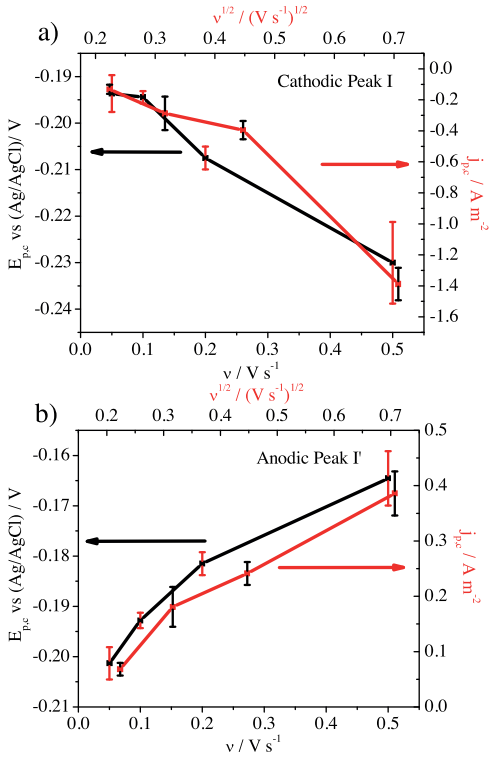

Fig. 5. Values for the cathodic peak I and anodic peak I' of rhenium oxides, electrodeposited by pulsed current using an electrolyte with 0.04 mol dm^{-3} ReO_4^- @ 50 A m^{-2}. Peak potential (E_p vs (Ag/AgCl)) as a function of scan rate (ν) and peak current density (j_p) as a function of square root of scan rate ($\nu^{-1/2}$). The voltammograms were recorded in 0.5 mol dm^{-3} H_2SO_4 electrolytes at 25 °C.

mechanism for the HER where the first step corresponds to a reduction of a metallic center according to Eq. (5), where the positive charge is replaced by the adsorption and intercalation of a proton, as shown in Eq. (6). The metallic center of Re is still able to reduce, as shown by Eq. (7). In order to compensate for the loss of a positive charge (through Re reduction) a proton is adsorbed and intercalated, as shown by Eq. (8). As a consequence, the two adsorbed protons come into contact and, by reduction, generate H_2 and regenerate the catalyst $(ReO_4)^-$, as expressed by Eq. (9). Similar to what was said for materials obtained from an electrolyte with a concentration of 0.02 mol dm^{-3} ReO_4^-, these reactions proceed simultaneously to the reaction shown in Eq. (4).

$$(Re^{VII}O_4)^-_{(s)} + e^- \rightarrow (Re^{VI}O_4)^{-2}_{(s)} \quad (5)$$

$$(Re^{VI}O_4)^{-2}_{(s)} + H^+ \rightarrow (H^+_{ad}Re^{VI}O_4)^-_{(s)} \quad (6)$$

$$(H^+_{ad}Re^{VI}O_4)^-_{(s)} + e^- \rightarrow (H^+_{ad}Re^{V}O_4)^{-2}_{(s)} \quad (7)$$

$$(H^+_{ad}Re^{V}O_4)^{-2(s)} + H^+ \rightarrow (H^+_{ad2}Re^{V}O_4)^-_{(s)} \quad (8)$$

$$(H^+_{ad2}Re^{V}O_4)^-_{(s)} \rightarrow (Re^{VII}O_4)^-_{(s)} + H_{2(g)} \quad (9)$$

This mechanism involves two more steps tan the previous one. However, this does not exclude the possibility of a joint or synergic action of the Re $^{IV-VII}$ species which may then influence the electro catalysis of the HER. This event, added to the various morphologic characteristics of the electro deposited materials, has an effect on the rate of the HER (H^+/H_2) as will be presently shown. The proposed mechanism in Eqs. (1)–(3) and (5)–(9) hypothesized a possible reaction path through the HER over Re oxides electrode. From this is clear that no spectroscopic information of the reactions occurring during the process supporting this mechanism. However, it is worth mentioning that obtaining in situ spectroscopic information of the electrocatalysis process of rhenium oxide is a highly interesting challenge but not yet resolved. Thus this proposed mechanism aims to be a milestone in the elucidation of the electrocatalysis process over rhenium oxides electrode.

Taking into account that the rate of the HER is charge transfer controlled, Tafel equation was adjusted to the cathodic part of the cyclic voltammograms for cathodic over potentials lower than −200 mV ($\eta < -200$ mV). In this fashion, it was possible to determine the exchange current density (j_0) of the HER for each one of the electrodeposited materials, as shown in Table 4. The electrocatalytic effect mentioned in a previous section was thus quantified, which made it evident that there is a clear distinction between the exchange current density on the electrodeposited materials as compared with its value on the ITO substrate (an increase of one order of magnitude). The exchange current density gave similar magnitude to values reported for solid electrodes of Re (7.24×10^{-2} A m^{-2}) and of Au ($0.31–31.60 \times 10^{-2}$ A m^{-2}) [11]. Among the electrodeposited materials it may be observed that those obtained from an electrolyte with a concentration of 0.04 mol dm^{-3} ReO_4^-, exhibit a greater j_0 value than those obtained from an electrolyte with a concentration of 0.02 mol dm^{-3} ReO_4^-. This result is a consequence of the greater amount of Re oxides on the surface of the electrodeposited material, as well as of the reduction of space between the 'islands' (nuclei of electrodeposited material) and the increase in grain size of the electrodeposits produced from an electrolyte with a concentration of 0.04 mol dm^{-3} ReO_4^- when compared to deposits obtained from an electrolyte of 0.02 mol dm^{-3} ReO_4^-.

Electrodeposited materials from electrolytes with a concentration of 0.02 mol dm^{-3} ReO_4^-showed a 'dispersed islands' morphology with a lower average Re concentration, lower rugosity, lower grain size and lower Re(VII) concentration in comparison with deposits from a 0.04 mol dm^{-3} ReO_4^- solution. Rugosity estimations by means of Atomic Force Microscopy (AFM) have shown that electrodeposits obtained from a 0.02 mol dm^{-3} ReO_4^- solution had an average roughness (Ra) between 11 to 17 nm, while electrodeposits obtained from a 0.04 mol dm^{-3} ReO_4^- solution had an average roughness (Ra) between 16 to 23 nm (data not shown for the sake of brevity). Rugosity plays an important role in electrocatalysis, because it defines the form of the diffusion profile of the H^+ and H_2 species in the electrolyte-catalytic surface interface. The smoother the sample, the lower the surface area and

Table 4
Kinetic parameters of the HER on rhenium oxides electrodes electro deposited by pulsed current in acidic medium at 25 °C (Scan rate ν = 10 mV s^{-1}).

Electrodeposit	Electrolyte	Cathodic Parameter	j_0 [A m^{-2}]	α	η_{1000} [V]
1	(0.02 mol dm^{-3} ReO_4^-)	(jc = 10 A m^{-2})	0.019 ± 0.001	0.451 ± 0.005	−0.620 ± 0.003
2		(jc = 50 A m^{-2})	0.024 ± 0.002	0.406 ± 0.005	−0.605 ± 0.003
3	(0.04 mol dm^{-3} ReO_4^-)	(jc = 10 A m^{-2})	0.021 ± 0.001	0.574 ± 0.005	−0.482 ± 0.001
4		(jc = 50 A m^{-2})	0.027 ± 0.002	0.493 ± 0.005	−0.549 ± 0.003
Bare ITO			0.008 ± 0.001	0.084 ± 0.001	−3.577 ± 0.030

the diffusion front behaves smoothly, whereas disperse nuclei present their own diffusion profile depending on their shape. This results in a distribution of proton diffusion profiles that, jointly, may diminish the process rate and increase the over potential required for the HER [15].

The values for the charge transfer coefficient (α) were estimated, as shown in Table 4. This coefficient is a geometry factor linked to the relative position of the Gibbs free energy curves corresponding to reactants and products in an electrochemical reaction [15]. It is then understood that the α parameter may take up values between 0 and 1, which shows that equilibrium may be displaced towards reactants or products, respectively. It is important to underline that the α values exhibited by the HER reaction on the electrodeposited materials are higher than those exhibited by the reaction on the ITO substrate, whose value is close to zero.

Finally, Table 4 shows the over potential necessary to reach a current density of 1000 A m^{-2} (η_{1000}) for the HER on each one of the studied surfaces. These values were calculated taking into account the previously reported kinetic parameters (j_0 y α). The determination of these values is important because they allow understanding, for instance, of the way the cathodic half-cell would operate in the process of water splitting or electrohydrolysis for the production of H_2. The ITO surface shows that a high over potential value is required to reach a considerable HER rate, which reaffirms the ideally polarizable electrode behavior previously discussed. The electrodeposited materials showed a better behavior in terms of the required over potential to reach a rate of 1000 A m^{-2} for the HER. In particular, it is to be noticed that the electrodeposited materials which arose from an electrolyte with a concentration of 0.04 mol dm^{-3} ReO_4^- exhibit a better effect on the electrocatalysis of the HER, where best results were obtained with a material which was electrodeposited at a cathodic current density of 10 A m^{-2}.

4. Conclusions

Using electrodeposition with periodic current reversal and varying the concentration of the ReO_4^- ion, Re oxides with a grain size of 200–500 nm were obtained on ITO. The increase in the concentration of the ReO_4^- ion caused an increase in the amount of Re in the deposit, due to an improvement of mass transfer in the electrocrystallization process. On the other hand, an increase in the cathodic current density favors progressive nucleation instead of instantaneous nucleation of the electrodeposited material, due to a higher availability of charge per unit area on the electrode surface. It is then possible to adjust the composition and morphology of the electrodeposit by varying the concentration of the ReO_4^- ion and the cathodic current density according to the requirements of HER electrocatalysis.

The Re oxide electrodeposits, which exhibited island shapes, showed an electrocatalytic behavior for the HER which was a function of their chemical composition and morphological characteristics, which can be compared to the behavior or smooth-surfaced Re and Au electrodes reported in the literature. The Re^{VII}/Re^{IV} ratio of Re species in the electrodeposit exhibited an influence on the HER electrocatalysis process. A greater abundance of the Re^{VII} species would cause a greater HER rate than that generated by the Re^{IV} species. Two possible electrocatalysis mechanisms were postulated that depend on the dominant species on the surface of the electrodeposit. The first mechanism was presented in reactions 1 to 4, where Re^{IV} would be the dominant species whereas equations 5 to 9 present a second mechanism which considers Re^{VII} as dominant species.

The electrocatalytic behavior of the electrodeposited materials is linked to Re concentration and electrodeposit morphology. The electrodeposit obtained at a ReO_4^- concentration of 0.04 mol dm^{-3} at a current density of 10 A m^{-2} exhibited the best electrocatalytic properties towards the REH (H^+/H_2). As a function of the η_{1000} parameter, an improvement of between 17 and 32% was observed in comparison with the other three electrodeposited materials. From the cyclic voltammograms recorded at a ReO_4^- ion concentration of 0.04 mol dm^{-3} with current density of 10 and 50 A m^{-2}, it was found that these electrodeposits may intercalate protons (H^+ ions). This behavior, apart from contributing to a better performance towards the HER, may open the possibility of using the electrodeposit as a supporting material for Mo and W oxides in electrochromic applications.

Acknowledgments

This research was supported by the CONICYT Chilean Research Agency via FONDECYT No. 1110116 project, headed by Prof. L. Cifuentes. Thanks are due to MOLYMET S.A. for providing the valuable NH_4ReO_4 used in the present work. A. Vargas-Uscategui specially thanks CIMAT, Materials Science Doctoral Program of FCFM-Universidad de Chile and MOLYMET S.A. for his Ph.D. scholarship. The authors would also like to thank the Mining Engineering Department (Universidad de Chile) for its continued support.

Appendix A. Supplementary data

Supplementary data associated with this article can be found, in the online version, at http://dx.doi.org/10.1016/j.electacta.2015.08.065.

References

[1] E. Cazzanelli, M. Castriota, S. Marino, N. Scaramuzza, J. Purans, A. Kuzmin, et al., Characterization of rhenium oxide films and their application to liquid crystal cells, J. Appl. Phys. 105 (2009) 114904, doi:http://dx.doi.org/10.1063/1.3138812.
[2] H.G. Nadler, F. Rhenium, Habashi Handb. Extr. Metall, Wiley-VCH Verlag GmbH & Co. KGaA, Weinheim Germany, 19971491–1501.
[3] M. Castriota, E. Cazzanelli, G. Das, R. Kalendarev, A. Kuzmin, S. Marino, et al., Proton presence and motion in rhenium-oxide films and their application to liquid-crystalline cells, Mol. Cryst. Liq. Cryst. 474 (2007) 1–15, doi:http://dx.doi.org/10.1080/15421400701693435.
[4] H.I. Karan, K. Sasaki, K. Kuttiyiel, C.a. Farberow, M. Mavrikakis, R.R. Adzic, Catalytic Activity of Platinum Monolayer on Iridium and Rhenium Alloy Nanoparticles for the Oxygen Reduction Reaction, ACS Catal. 2 (2012) 817–824, doi:http://dx.doi.org/10.1021/cs200592x.
[5] J. Tayal, B. Rawat, S. Basu, Effect of addition of rhenium to Pt-based anode catalysts in electro-oxidation of ethanol in direct ethanol PEM fuel cell, Int. J. Hydrogen Energy 37 (2012) 4597–4605, doi:http://dx.doi.org/10.1016/j.ijhydene.2011.05.188.
[6] S. Escolastico, J. Seeger, S. Roitsch, M. Ivanova, W. a Meulenberg, J.M. Serra, Enhanced H2 separation through mixed proton-electron conducting membranes based on La5.5 W0.8 M0.2 O11. 25-δ, ChemSusChem 6 (2013) 1523–1532, doi:http://dx.doi.org/10.1002/cssc.201300091.
[7] E.C. Muñoz, R.S. Schrebler, M.A. Orellana, R. Córdova, Rhenium electrodeposition process onto p-Si(100) and electrochemical behaviour of the hydrogen evolution reaction onto p-Si/Re/0. 1M H2SO4 interface, J. Electroanal. Chem. 611 (2007) 35–42, doi:http://dx.doi.org/10.1016/j.jelechem.2007.07.023.
[8] E.C. Muñoz, R.S. Schrebler, P.C. Grez, R.G. Henríquez, C.A. Heyser, P.A. Verdugo, et al., Rhenium electroless deposition on p-Si(100) from HF solutions under illumination: Hydrogen evolution reaction onto p-Si/Re systems, J. Electroanal. Chem. 633 (2009) 113–120, doi:http://dx.doi.org/10.1016/j.jelechem.2009.05.001.
[9] X. Yang, B.E. Koel, H. Wang, W. Chen, R. a Bartynski, Nanofaceted C/Re(1121): fabrication, structure, and template for synthesizing nanostructured model Pt electrocatalyst for hydrogen evolution reaction, ACS Nano 6 (2012) 1404–1409, doi:http://dx.doi.org/10.1021/nn204615j.
[10] R. Brimblecombe, G.C. Dismukes, G.F. Swiegers, L. Spiccia, Molecular water-oxidation catalysts for photoelectrochemical cells, Dalt. Trans. (2009) 9374–9384, doi:http://dx.doi.org/10.1039/b912669d.
[11] M.R. Tarasevich, O.V. Korchagin, Electrocatalysis and pH: A review, Russ. J. Electrochem. 49 (2013) 600–618, doi:http://dx.doi.org/10.1134/S102319351307015X.
[12] S. Szabó, I. Bakos, Study of rhenium deposition onto Pt surface with electrochemical methods, in: B. Delmon, P.A. Jacobs, R. Maggi, A. Martens, J.P.

Grange, G. Poncelet (Eds.), Prep. Catal. VII, Proc. 7th Int. Symp. Sci. Bases Prep. Heterog. Catal., Elsevier Science B.V., Louvain-la-Neuve, Belgium, 1998, pp. 269–276, doi:http://dx.doi.org/10.1016/S0167-2991(98) 80191-2.
[13] S. Szabó, I. Bakos, Rhenium as an accelerator of iron corrosion, Corros. Sci. 43 (2001) 931–938, doi:http://dx.doi.org/10.1016/S0010-938X(00)00110-4.
[14] D. Shirley, High-resolution X-ray photoemission spectrum of the valence bands of gold, Phys. Rev. B 5 (1972) 4709–4714, doi:http://dx.doi.org/10.1103/PhysRevB.5.4709.
[15] A.J. Bard, L.R. Faulkner, Electrochemical methods: fundamentals and applications, 2nd ed., John Wiley & Sons, Inc., New York, NY, 2001.
[16] D. Marin, F. Medicuti, C. Teijeiro, An Electrochemistry Experiment: Hydrogen Evolution Reaction on Different Electrodes, J. Chem. Educ. 71 (1994) A277, doi:http://dx.doi.org/10.1021/ed071pA277.
[17] A. Vargas-Uscategui, E. Mosquera, L. Cifuentes, Transmission electron microscopy study of electrodeposited rhenium and rhenium oxides, Mater. Lett. 94 (2013) 44–46, doi:http://dx.doi.org/10.1016/j.matlet.2012.12.005.
[18] A. Vargas-Uscategui, E. Mosquera, L. Cifuentes, Analysis of the electrodeposition process of rhenium and rhenium oxides in alkaline aqueous electrolyte, Electrochim. Acta 109 (2013) 283–290, doi:http://dx.doi.org/10.1016/j.electacta.2013.07.091.
[19] J. Okal, J. Baran, Laser Raman Characterization of Oxidized Re/γAl2O3Catalysts: Effect of Calcination Temperature, J. Catal. 203 (2001) 466–476, doi:http://dx.doi.org/10.1006/jcat.2001.3340.
[20] W.T. Tysoe, F. Zaera, G.A. Somorjai, An XPS study of the oxidation and reduction of the rhenium-platinum system under atmospheric conditions, Surf. Sci. 200 (1988) 1–14, doi:http://dx.doi.org/10.1016/0039-6028(88)90428-1.
[21] E.S. Shpiro, V.I. Avaev, G.V. Antoshin, M.A. Ryashentseva, K.M. Minachev, XPS studies of the rhenium state in supported Re catalysts, J. Catal. 55 (1978) 402–406, doi:http://dx.doi.org/10.1016/0021-9517(78)90227-0.
[22] B.P. Hahn, R.A. May, K.J. Stevenson, Electrochemical deposition and characterization of mixed-valent rhenium oxide films prepared from a perrhenate solution, Langmuir 23 (2007) 10837–10845, doi:http://dx.doi.org/10.1021/la701504z.
[23] A. Vargas-Uscategui, E. Mosquera, J.M. López-Encarnación, B. Chornik, R.S. Katiyar, L. Cifuentes, Characterization of rhenium compounds obtained by electrochemical synthesis after aging process, J. Solid State Chem. 220 (2014) 17–21, doi:http://dx.doi.org/10.1016/j.jssc.2014.07.043.
[24] J. Okal, W. Tylus, L. Kepinski, XPS study of oxidation of rhenium metal on?-Al2O3 support, J. Catal. 225 (2004) 498–509, doi:http://dx.doi.org/10.1016/j.jcat.2004.05.004.
[25] A. Guerfi, R.W. Paynter, L.H. Dao, Characterization and Stability of Electrochromic MoO3 Thin Films Prepared by Electrodeposition, J. Electrochem. Soc. 142 (1995) 3457–3464, doi:http://dx.doi.org/10.1149/1.2050004.
[26] S.-I. Ho, D.P. Whelan, K. Rajeshwar, Electrocatalytic Modification of Indium Tin Oxide Electrode Surfaces, J. Electrochem. Soc. 135 (1988) 1452–1457, doi:http://dx.doi.org/10.1149/1.2096023.
[27] C.G. Granqvist, Hanbook of inorganic electrochromic materials, 2 ed., Elsevier Science B.V., Amsterdam, 2002.
[28] D. Pletcher, R. Greff, R. Peat, L.M. Peter, Instrumental methods in electrochemistry, Woodhead Publishing, Southampton, 2001.